Theory of Microphase Separation in Block Copolymer/ Homopolymer Mixtures

A. E. Likhtman[†] and A. N. Semenov[*,†,‡]

Physics Department, Moscow State University, Moscow 117234, Russia, and Department of Applied Mathematical Studies, University of Leeds, Leeds LS2 9JT, U.K.

Received February 27, 1997; Revised Manuscript Received July 28, 1997[⊗]

ABSTRACT: We present a theory of microphase separation of a diblock copolymer $A_{fN}B_{(1-f)N}$ and homopolymer hB blend in the strong segregation limit ($\chi N \gg 10$), where χ is the Flory−Huggins interaction parameter. Homopolymer chains are assumed to be much longer than block copolymers: $N_h \gg N$. In this case, homopolymers and diblock copolymers are separated in each elementary cell. We derive a general equation for the free energy and calculate it numerically for different microdomain superstructures: classical lamellar, hexagonal, and body-centered cubic (BCC) structures and also bicontinuous OBDD and gyroid structures. As a result, a phase diagram is constructed in coordinates (f, φ), where f is the diblock copolymer composition and φ is the volume fraction of the homopolymer in the blend. In particular, we predict a region of stability of one of the bicontinuous phases in the composition window, $f = 0.62-0.66$.

1. Introduction

Diblock copolymers attract significant interest due to their ability to form periodic spatial superstructures.[1] A diblock copolymer molecule consists of two chemically connected different blocks (A and B). At appropriate conditions (usually at low enough temperatures) the blocks separate and form a microdomain structure if the Flory−Huggins interaction parameter $\chi_{AB} \equiv \chi(T)$ exceeds some critical value χ^* (a macrophase separation in monodisperse copolymer melts is suppressed by chemical junctions between A and B blocks). Leibler's theory[2] predicts $\chi^* \simeq 10.5/N$, where $N = N_A + N_B$ is the total number of monomers per diblock copolymer chain. In the weak segregation regime corresponding to a vicinity of χ^* (i.e., $\chi/\chi^* - 1 \ll 1$), the boundaries between A and B domains are very smooth. In the opposite regime, $\chi N \gg 10$ (strong segregation limit), the interdomain boundaries are sharp and A and B blocks are well segregated: the fraction of A monomers in a B domain is small and vice versa.

The geometry and the period of superstructures are determined by competition of two factors: effective repulsion of A and B monomers and stretching of copolymer chains required in order to satisfy the incompressibility condition. Traditionally, three structures were considered first:[1,2] In the symmetric case $f \approx 0.5$, the system forms a lamellar structure (lam), which consists of flat A and B layers. As the block copolymer composition becomes more asymmetric, the structure transforms to an array of hexagonally packed A cylinders in a B matrix (if $f \equiv N_A/N < 0.5$) or to a BCC (body-centered cubic) lattice of spherical domains.[2,3] In the strong segregation limit, the morphology is determined by the composition f only, while in general it is also temperature dependent (via $\chi(T)$ dependence).

Novel superstructures observed more recently in different copolymer systems[4−8] include ordered bicontinuous double diamond (OBDD) structure (space symmetry group $Pn3m$), the gyroid structure ($Ia3d$), and also the modulated and perforated lamellar phases. The OBDD implies two interpenetrating diamond lattices of minor component inside the matrix of the major component. A detailed analysis of experimental data[9] led to the conclusion that the observed bicontinuous structure was a gyroid $Ia3d$ structure also consisting of two interpenetrating networks of minor component. All novel phases were found in the narrow composition range between lamellar and hexagonal phases. Several theoretical approaches[10−12] based on the strong segregation theory[3] showed that OBDD structure is not stable for a strongly segregated pure diblock copolymer melt. One can expect also a similar instability of the gyroid phase due to its similarity to the OBDD.

An addition of a homopolymer hB, which is chemically identical to one of the copolymer blocks, can significantly influence the equilibrium structure.[13−19] Diblock/homopolymer mixtures exhibit both macro- and microphase separation. The additional macroscopic parameters, homopolymer volume fraction $\varphi = V_{hB}/V$ and homopolymer molecular weight, can be adjusted to produce a different structure.

In this paper we extend the previous approach[10] to the case of diblock/homopolymer mixtures and consider traditional and bicontinuous phases.

We analyze the validity of the round elementary cell approximation used before[13] and find the regions in (f, φ) coordinates where this approximation is accurate.

We also propose a general method that allows us to calculate the free energy for an arbitrary shape of the elementary cell. This approach is then applied to various classical and bicontinuous phases. The interfacial geometry is determined by direct minimization of the free energy. The resultant (f, φ) phase diagram is discussed in section 5.

2. Theory

We consider a diblock copolymer with $N = N_A + N_B$ monomers and assume that statistical segments (a_{st}) of A and B blocks are equal. We also assume that A and B monomer volumes are equal: $v_A = v_B = v$ and consider k_BT and v as the energy and volume units correspondingly. The free energy of a diblock copolymer melt in the strong segregation limit ($\chi N \gg 10$) (of course, we also assume that the copolymer chains are long: $N \gg 1$) can be represented as a sum of two main contribu-

[†] Moscow State University.
[‡] University of Leeds.
[⊗] Abstract published in *Advance ACS Abstracts,* September 15, 1997.

S0024-9297(97)00271-4 CCC: $14.00

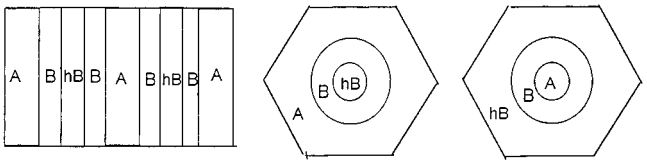

Figure 1. Example of the microphase separation in diblock copolymer (AB)/homopolymer (hB) mixture. Lamellar and two possible hexagonal structures.

tions, interfacial energy (F_i) and elastic energy due to elongation of block copolymer chains (F_{el}):[3]

$$F = F_i + F_{el} \tag{1}$$

where

$$F_i = \gamma S \tag{2}$$

γ is the interfacial tension and S is the surface area of the A/B interface. The surface tension is[20−22]

$$\gamma = \gamma_{AB} = a\chi^{1/2} \tag{3}$$

where $a = a_{st}/\sqrt{6}$.

Let us now consider a mixture of AB diblock copolymer and homopolymer (hB) for the limit of long homopolymer chains: $N_h \gg N$. Note that in the strong segregation limit long homopolymers must separate from diblock copolymers since an insertion of an hB chain inside a region filled by stretched B blocks would significantly increase the elastic energy of the block elongation. So, in this case, each elementary cell is divided into three regions by two interfaces: the regions of A and B blocks and the homopolymer region. An example of this separation is shown in Figure 1.

The tension of the hB/B interface is small (in comparison with $\gamma = \gamma_{AB}$) since B monomers only (which are essentially indifferent to each other) are involved. Hence in the main approximation the contribution of hB/B interfaces to the free energy can be neglected. Thus the free energy of the AB/hB mixture is still defined by eq 1 with F_e being the copolymer elongation energy (note that homopolymer chains need not be elongated), and F_i, the energy of A/B interfaces.

Let us consider the elastic energy first for the case of flat (lamellar) copolymer layers:

$$F_{el} = F_{el}^{A} + F_{el}^{B} \tag{4}$$

where $F_{el}^{A,B}$ is the contribution of A and B blocks correspondingly,

$$F_{el}^{A}[\mathbf{r}] = \sum_{[A]} \int_0^{N_A} \frac{1}{4a^2} \left(\frac{\partial \mathbf{r}_n}{\partial n}\right)^2 \mathrm{d}n \tag{5}$$

and an analogous equation is valid for B blocks. Here [A] denotes all A blocks, and $\mathbf{r}_n$ is a position of the nth link of an A block ($n = 0$ corresponds to the junction point, $n = N_A$ to the free end of the block). The elastic free energy, eq 5, should be minimized for a given overall distribution of A links: $\phi_A = 1$ inside A domains and $\phi_A = 0$ otherwise.

This minimization was performed using the method of Lagrangian multipliers; the result is[10]

$$F_{el}^{A} = \frac{\pi^2}{16} \frac{1}{N_A{}^2 a^2} \int_{[A]} z^2(\mathbf{r})\, \mathrm{d}^3\, \mathbf{r} \tag{6}$$

where the integration is performed over the volume of all A domains and $z(\mathbf{r})$ is the distance from the point $\mathbf{r}$ to the nearest A/B interfacial plane.

Let us return to the general case of an arbitrary (nonlamellar) structure with curved interfaces. It is easy to check that eq 6 gives correct results for the elastic free energy of inner parts of cylindrical and spherical domains (see refs 3 and 10).

The above treatment involves two approximations:

(1) The free ends of A blocks are assumed to be distributed across the whole A domain (and the same is true for B blocks).

(2) We consider A and B blocks separately as two brushes grafted to the interface so that the grafted ends (which correspond to junction points) are free to move along the interface.

Let us discuss these assumptions. **The first assumption** is always valid for a lamellar structure, and also for isolated minor domains, e.g., for spherical and cylindrical domains. However, the assumption is not exactly valid for the outer (matrix) part of an elementary cell, i.e., for a brush grafted to, e.g., a cylinder, or a sphere from outside. In this case, a detailed analysis[3,23] shows the existence of narrow "dead zones" near the interface: the free chain ends are expelled from these zones. In this situation, eq 6 corresponds to a *formal* minimum of the elastic free energy, which, however, implies a negative density of free ends, ρ, in the "dead zone" near the cylinder[3,23] (note also that this formal minimum corresponds to the parabolic molecular potential). Thus with the additional physical condition $\rho \geq 0$, the formal minimum (eq 6) cannot be reached, so that the true elastic free energy must be higher: it corresponds to a physical end distribution which must be exactly equal to zero in a narrow excluded zone near the cylinder (the interface).[23] Therefore, in this case, eq 6 provides a lower boundary for the elastic free energy.

The relative difference between the true elastic energy and eq 6 depends on the interfacial curvature. For small curvatures this difference is exponentially small.[23] Moreover, using the result of ref 23, we showed that in the composition region of interest ($f \lesssim 0.7$)[24] the relative error of eq 6 is less than 0.06%; i.e., it is negligible.

The second assumption actually implies that the elastic free energies of A and B brushes are minimized separately. The blocks follow the shortest path between the free end and the grafting surface (i.e., interface) in order to minimize their degree of stretching. Therefore, the block paths are both straight and normal to the interface. Note, however, that in this case the distribution of grafted ends along the interface is governed by the geometry of the corresponding domain. The above picture is valid as long as the distributions of grafted ends of A blocks and B blocks are the same (remember that A and B blocks are actually connected in a common block copolymer chain, so that the concentrations of A and B grafted ends must coincide):

$$\sigma_A \equiv \sigma_B \tag{7}$$

where σ_A and σ_B are the surface concentrations of A and B blocks. This is true, for example, for a lamellar structure, when both distributions are uniform. However, this is not true in the general case of curved interfaces, as the geometries of A and B domains might dictate different distributions of grafted points.

Therefore, we have to minimize the elastic free energy, eq 4, under the additional constraint, eq 7,

which implies a coupling between the A and B brushes (this coupling can be expressed in terms of a molecular force acting on grafted A ends due to the B brush). As a result, the equilibrium block trajectories might become not straight, and not normal to the interface. In order to simplify the treatment, we will still assume that each block follows on the average a straight path, yet we allow for arbitrary orientations of these paths. Thus we define the block conformations by the *block orientation field*, i.e., by defining the block orientation $\mathbf{n}_A(u,v)$ at each point at the interface, (u, v). Both the elastic free energy of the A brush and the surface distribution, $\sigma_A(u,v)$, are determined by the block orientation field $\mathbf{n}_A(u,v)$. The elastic free energy $F_{el}^A[n_A(u,v)]$ can be calculated using eq 6. However, we should take into account that the blocks are stretched along the lines determined by the orientation field, i.e., that $z(\mathbf{r})$ is now defined as the distance from point $\mathbf{r}$ to the interface *along the chain path* that is parallel to $\mathbf{n}_A(u,v)$, where (u, v) is the destination point at the interface. The total elastic free energy F_{el} can be obtained as a result of minimization of $F_{el}^A[n_A(u,v)] + F_{el}^B[n_B(u,v)]$ over the block orientation fields $\mathbf{n}_A$ and $\mathbf{n}_B$ under the condition 7. This condition can be represented in a bit different way: By virtue of incompressibility, $\sigma_A = V_A/(N_A\Delta A)$, where V_A is the partial volume "shaded" by the A blocks attached to the interfacial element ΔA, and a similar equation defines σ_B. Hence, we get the following condition on the partial volumes:

$$V_A/V_B = N_A/N_B = f/(1-f) \tag{8}$$

Thus the block orientation fields are not known a priori: it is determined by the minimization procedure, which is described in more detail in section 4; in particular, we show how to parametrize the block orientation fields in terms of surface "potentials".

Using eqs 1−4 and 6, we write the free energy of a diblock/homopolymer blend (per one diblock copolymer chain):

$$F = Na\chi^{1/2}\frac{S_0}{V_{AB}} + \frac{\pi^2}{16}\frac{1}{Na^2V_{AB}}\left\{\frac{1}{f^2}\int_{[A]} z^2(r)\, d^3r + \frac{1}{(1-f)^2}\int_{[B]} z^2(r)\, d^3r\right\} \tag{9}$$

where $V_{AB} = (1-\varphi)V_0$ is the volume occupied by diblock copolymers in a Wigner−Seitz cell V_0, S_0 is the interfacial (A/B) area per cell, and $\int_{[A],[B]}$ mean integrals over the the regions occupied by A and B blocks (note that $[A] + [B] = V_{AB}$).

For a given morphology, the free energy (9) should be minimized over the period (linear size of the elementary cell) L. It easy to see that for all structures the free energy terms (interfacial and elongational) scale as

$$F_i \sim \frac{1}{L}; \qquad F_{el} \sim L^2 \tag{10}$$

So minimization over L is trivial:

$$F = (\chi N)^{1/3}\tilde{F}(f) \tag{11}$$

where $\tilde{F}(f)$ is a numerical factor

$$\tilde{F}(f) = \frac{3}{2^{2/3}}\left\{\frac{\pi^2}{16}\frac{S_0^{\,2}}{V_{AB}^{\,3}}\left[\frac{1}{f^2}\int_{[A]} z^2(r)\, d^3r + \frac{1}{(1-f)^2}\int_{[B]} z^2(r)\, d^3r\right]\right\}^{1/3} \tag{12}$$

The equilibrium period is

$$L = N^{1/2}a(\chi N)^{1/6}\tilde{L}(f) \tag{13}$$

where $\tilde{L}(f)$ is another numerical factor.

3. Geometry of the Structures

To evaluate the integrals in eq 12, we need to know the shape of the two interfaces (A/B and B/hB) and the field of block orientations. The answers are obvious for the lamellar structure due to its symmetry. Hence we easily get $\tilde{F}_{lam} = (3\pi)^{2/3}/4$. Note that $\tilde{F}_{lam}$ does not depend on f and φ. All previous calculations for cylindrical and spherical structures were based on the assumption of the round elementary cell. With this assumption, all interfaces should also be round (because of the symmetry) and all blocks should be oriented radially. In this case, all integrals in eq 12 are trivial.

Since our aim is to build the phase diagram for all f and φ and also include the bicontinuous phases, we cannot use the assumption of the round elementary cell (below we show that the differences between the free energies of different structures are very small, so a very high precision is required in order to discriminate them). In particular, it is obvious that for the case $f < 0.5$ and small φ one of the interfaces is close to the boundary of the elementary cell and the assumption of the round cell becomes inappropriate. So it is necessary to calculate the free energies of traditional structures with true elementary cells, which are shown in Figures 1 and 2 (actually, we consider only the minimal symmetry element of the cells, 1/12 part for the hexagonal and 1/48 part for the BCC structures).

Let us describe now two bicontinuous structures: ordered bicontinuous double diamond (OBDD) and gyroid. Each of them consists of two interpenetrating networks of the minor component inside the matrix of the major component. One of these networks and its elementary cell part are shown in Figure 3.

One can construct the OBDD structure in the following way. First let us construct a single diamond lattice. It consists of 4-fold elements with one end of each rod in the center and another at the apexes of a symmetric tetrahedron. A neighboring element can be obtained by reflecting the first element at a rod end. The second

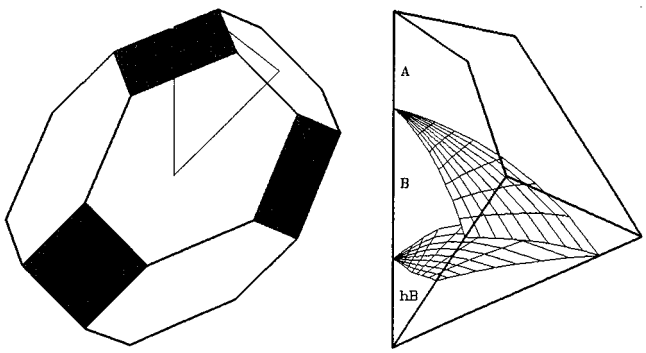

Figure 2. Elementary cell of the BCC structure (left), its minimal element (1/48 part) and the calculated interfaces (right).

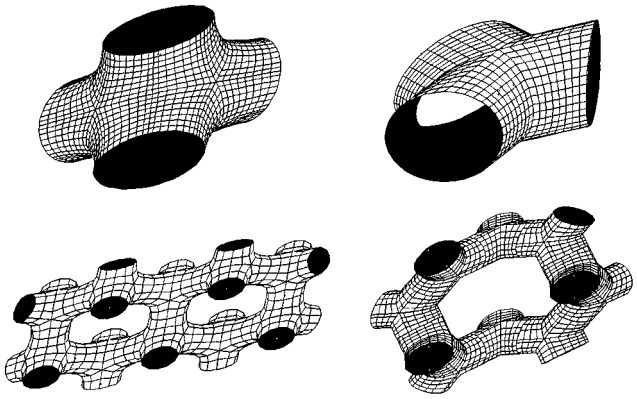

Figure 3. Calculated A/B interfaces and the elementary cell for OBDD (left) and gyroid (right) structures. One network only is shown.

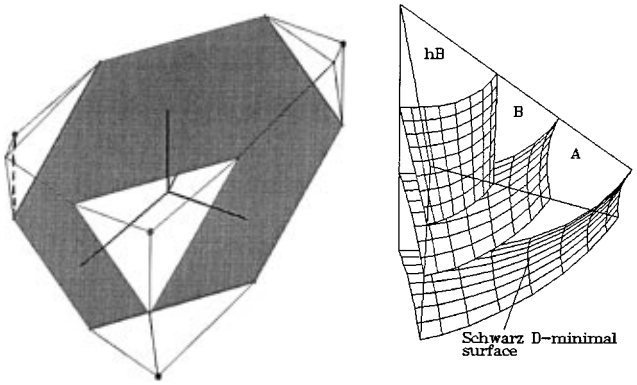

Figure 4. Elementary cell of a single diamond lattice (left), half of its minimum element (1/24 part) and the calculated interfaces (right).

lattice is a mirror reflection image of the first one. The minor component in a pure diblock copolymer system accumulates in the vicinity of each lattice. A homopolymer hB added to block copolymers with minor B block forms inner parts of two networks that are covered by blocks B and are immersed in the A matrix. The matrix itself consists of two parts filled by A blocks "grafted" to two different B networks. We assume that the A/A interface separating these two parts coincides with a Schwarz D-surface, a triply periodic surface with zero mean curvature dividing the space into two congruent subvolumes. The elementary cell of a single diamond structure and half of its minimum symmetry element (1/24 part) limited by the Schwarz surface are shown in Figure 4.

The gyroid structure looks similar to the OBDD. Each of the skeleton lattices is based on a 3-fold element, consisting of three rods with one end in the center and another at an apex of a symmetric triangle. In order to produce a neighboring element, one should rotate the priming element around the *AB* axis by 180° (see Figure 5) and then rotate it around the *OA* axis at the angle $\theta_g = 70.5288°$.

This procedure leads to a single gyroid lattice; the second lattice is a reflection of the first one. The A/A interface is assumed to be given by the zero-mean-curvature surface with the symmetry of the gyroid, the Schoen minimum G-surface.[25] The gyroid lattice is less symmetric than the OBDD: the elementary cell can be divided only into six equivalent parts (it has rotational symmetry elements only). The elementary cell and its minimal element limited by a Schoen G-surface are shown in Figure 6.

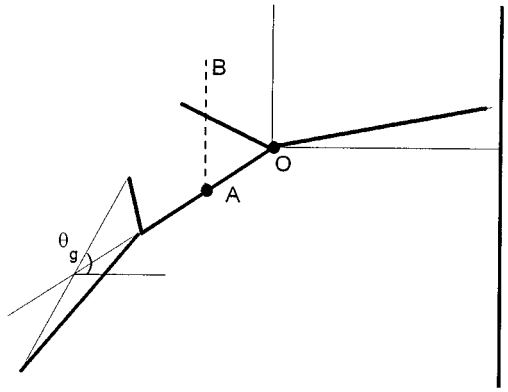

Figure 5. Schematic construction of a single gyroid lattice.

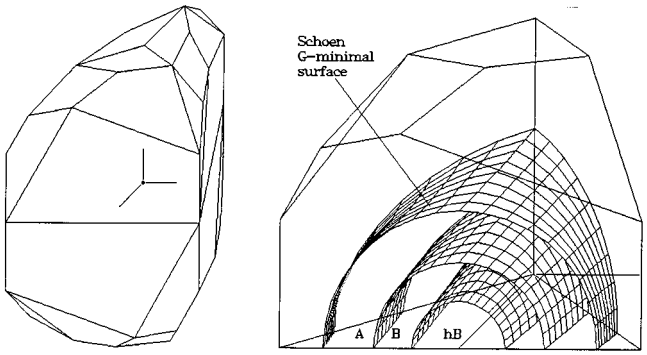

Figure 6. Elementary cell of a single gyroid lattice (left), half of its minimum element (1/6 part) and the calculated interfaces (right).

4. Free Energy Calculation

In this paper we do not assume any particular interfacial shape, nor do we assume any a priori orientations of polymer blocks. In order to determine these objects, we use the following minimization procedure: First of all, we divide the minimal element of the structure into a set of wedges using a set of straight lines. Then we define the interfaces by setting the points of the intersections between these lines and the interfaces. So we describe interfaces by two functions of two variables $k_{A/B}(i,j)$ and $k_{B/hB}(i,j)$, where i and j are the line numbers. After that, we define the orientations of blocks A in the following way.[26]

We assume that a chain, passing by the point **r**, is "attached" to the point (u, v) on the A/B interface, which corresponds to the minimum of the function $z(\mathbf{r},u,v) + g_A(u,v)$, where $z(\mathbf{r},u,v)$ is the distance between the points **r** and (u, v) and $g_A(u,v)$ is an unknown function (surface "potential") that determines deviations of orientations of A blocks from the normals to the A/B interface (note that $g_A(u,v) = 0$ corresponds to the normal orientation of the blocks assumed in our previous work[10]). The orientations of the B blocks are defined in a similar way. Thus the interfacial shapes and the block orientation fields are determined by four functions, $k_{A/B}$, $k_{B/hB}$, g_A, and g_B, which in turn are defined by minimization of the free energy functional F, eqs 11 and 12, under the additional constraint (8) (note that V_A and V_B are the geometrical objects defined by the interfacial shapes):

$$F(f,\varphi) = \min_{V_A/V_B(u,v)=f/(1-f)} F(k_{A/B}(i,j),k_{B/hB}(i,j),g_A(u,v),g_B(u,v))$$

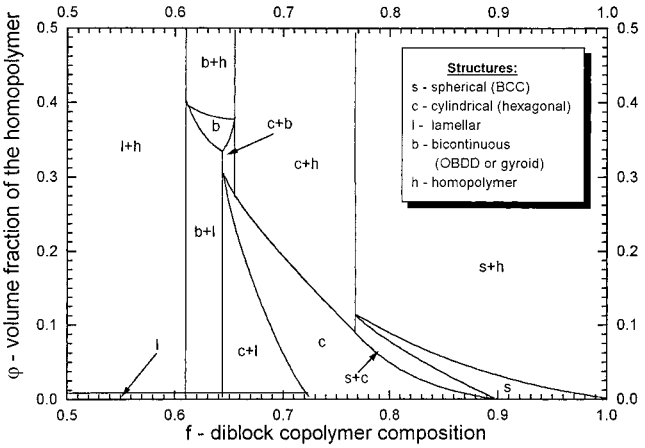

Figure 7. Phase diagram of a block copolymer/homopolymer mixture.

5. Results and Discussion

Using the approach described above, we calculate the free energies of BCC, hexagonal, OBDD, and gyroid structures for $f = 0.5-1$ and for $\varphi = 0-1$. Condition $f > 0.5$ means that we always consider the case when the hB homopolymer is added to the minority component. In the opposite case, $f < 0.5$, it is easy to show that the free energies of the traditional phases do not depend on φ for $\varphi \gtrsim 0.05$(and with the assumption of a round elementary cell they do not depend on φ at all). So the (f, φ) phase diagram in this case includes vertical lines only, which divide the regions where traditional phases are in equilibrium with a pure homopolymer phase (see ref 13; note that according to our results the bicontinuous phases are not stable in the strong segregation limit for $f < 0.5$).

We found that for all compositions and for all morphologies the free energy per block copolymer chain shows a minimum as a function of homopolymer volume fraction at some $\varphi = \varphi_m$ (except for the lamellar structure: the corresponding free energy is independent of φ). An addition of a small amount of homopolymer always results in a free energy decrease related to the fact that homopolymer fills those parts of a B domain that are remote from the A/B interface, thus allowing the B blocks to shrink a bit. The corresponding decrease of the elastic free energy of B blocks is more significant than an increase of the interfacial energy due to a partial swelling of B domains by the homopolymer (i.e., due to an interfacial area increase).

On the other hand for a large $\varphi > \varphi_m$ an increase of the interfacial area is a dominant factor. Hence for $\varphi > \varphi_m$ it is energetically favorable for the system to separate into two macrophases: a microphase-separated block copolymer phase with $\varphi = \varphi_m$ and a pure homopolymer phase. So both micro- and macrophase separations are considered below.

The resultant phase diagram is shown in Figure 7. Note that the lines shown in this figure are *binodal* lines corresponding to phase equilibria between different macrophases. These lines are calculated in a standard way by comparing (homopolymer and/or block copolymer) osmotic pressures and chemical potentials in different phases. We use the following notations: A region marked as (s, c, ...) corresponds to a one-phase system (with spherical, cylindrical, etc. morphology). Phase separation (two macrophases) regions are denoted with the sign +. For example, s + h denotes a BCC structure in equilibrium with the pure homopolymer phase, and s + c corresponds to coexisting BCC and hexagonal superstructures.

The main features of the phase diagram are considered below. The horizontal axis $\varphi = 0$ corresponds to the case of a pure diblock copolymer. In this case, three classical morphologies (lamellar, hexagonal, and BCC) are predicted in corresponding composition windows; these are in agreement with analytical results of ref 3. Note that bicontinuous phases are never stable for $\varphi = 0$, in agreement with our previous result.[10]

An addition of homopolymer dramatically changes the situation, giving rise to a lot of new phases and their combinations. We found that the free energies of OBDD and gyroid superstructures are very close to each other in all the regimes (the relative difference is less than 1%). Hence a discrimination of these two phases turns out to be impossible with our approach. So below a bicontinuous phase means either OBDD or gyroid. These structures are stable in a narrow composition window $f = 0.62-0.66$ (note that this window agrees well with the region $f = 0.65-0.69$ where bicontinuous phases were observed for a polystyrene−polyisoprene diblock copolymer[27]) if the homopolymer volume fraction is moderate, $\varphi \approx 0.3-0.4$. For $\varphi < 0.3$, bicontinuous structures coexist with a lamellar structure; for $\varphi > 0.4$, they coexist with a homopolymer phase. Note that all structural changes take place for $\varphi < 0.4$ since φ_m is always less than 0.4. When the homopolymer volume fraction changes from 0 to 0.4, the structure changes in the following way: hex → hex + BCC → BCC → BCC + homopolymer for $f = 0.9-0.8$, or hex + lam → hex → hex + homopolymer for $f = 0.73-0.66$, or bicontinuous + lam → bicontinuous → bicontinuous + homopolymer for $f = 0.66-0.62$.

Thus we found that an addition of homopolymer always favors formation of a structure with larger mean curvature (i.e., the following sequence of transitions is induced by homopolymer: lam → bicontinuous → hex → BCC), in agreement with the results of ref 13. This tendency can be attributed to the fact that homopolymer hB swells minor B domains, thus relaxing the interfacial curvature and reducing the free energy of cylindrical and spherical structures (the reduction effect is more significant for a spherical morphology characterized by initially more curved interfaces). Note that essentially the same explanation of the homopolymer effect was suggested before.[13,16]

Note that we found a wider region of stability of the hexagonal structure than that predicted in ref 13. In particular, we see that the hexagonal phase can accommodate up to $\varphi \simeq 30\%$; the corresponding limiting φ calculated in ref 13 is much lower, in particular, due to the round elementary cell approximation adopted there.

Our analysis shows that the round elementary cell approximation is good if the amount of homopolymer is small: $\varphi \lesssim 5\%$. In this case the phase boundaries obtained with this approximation are accurate within the error of 20%. The round cell approximation is qualitatively invalid if $\varphi \gtrsim 10\%$.

Phase behaviors of copolymer/homopolymer blends including different equilibrium superstructures have been considered by Matsen.[16] However, the regimes considered in ref 16 correspond to (1) essentially weakly segregated structures and (2) homopolymer chains of lengths comparable with that of block copolymers: $\alpha = N_h/N \leq 1.5$. In contrast, our phase diagram is calculated in the strong segregation regime and for $N_h/N \gg 1$. Let us compare the phase diagram shown in Figure

7 of ref 16 (for the largest $\alpha = 1.5$) with our results (note a difference in definition of the composition f, which could be canceled by transformation $f \rightarrow 1 - f$). Both (f, φ) phase diagrams contain similar regions of pure lamellar, cylindrical, BCC, and bicontinuous phases. In particular, the region of bicontinuous phase is roughly a triangle located between lamellar and cylindrical domains. The main differences between the diagrams are (1) the lamellar domain is much larger in the weak segregation regime, (2) in the strong segregation regime a cylindrical phase can absorb a much larger amount of homopolymer (up to 30%) than for weak segregation (up to 5%), and (3) the regions of macrophase separation between two superstructures (cylindrical + lamellar, bicontinuous + lamellar, BCC + cylindrical) are negligible in the weak segregation diagram of ref 16 but are wide in the strong segregation regime.

Exactly the same system (diblock copolymer/homopolymer mixture in the strong segregation limit) was considered theoretically by Xi and Milner.[19] Their approach is similar to that developed in the present paper in many respects. However, the approximations of ref 19 are more severe: the theory is based on the round elementary cell approximation for classical morphologies, and on a similar "generic wedge" approximation for bicontinuous structures. However, it is precisely our point that the round elementary cell approximation is not good enough, especially if the homopolymer fraction is not small. The advantage of the present approach is that we allow for an arbitrary shape of both A/B and B/hB interfaces, and also for arbitrary orientations of the block trajectories with respect to the A/B interface; we also allow for different orientations of A and B blocks of the same copolymer (the free energy is minimized with respect to the corresponding parameters). The main conclusion of ref 19 is that bicontinuous phases are stable in the region $f = 0.56-0.68$ of block copolymer compositions, and also for homopolymer volume fractions ranging from $\varphi = 0.18$ to 1. Our prediction for the corresponding composition window is $f = 0.62-0.66$, i.e., close enough to the previous result. However, we predict that bicontinuous phases are stable in a narrow window of homopolymer fractions, $\varphi = 0.33-0.4$. For lower and for higher values of φ, the system is predicted to macrophase separate: one phase is bicontinuous, and the other is "classical" (or just almost neat homopolymer).

6. Summary

A generalized theory of microphase separation in diblock copolymer/homopolymer blends in the strong segregation limit is proposed in this paper. In particular, we lift the assumption of the round (spherical, cylindrical) elementary cell of a microdomain structure and also allow for arbitrary orientation of polymer chains (blocks). We show that long homopolymer chains added to the minority block copolymer component may induce a morphological change from lamellar to bicontinuous structure or lamellar to cylindrical or cylindrical to spherical. We also find wide regions of macrophase separation between a disordered homopolymer phase and a superstructure or between two superstructures.

Acknowledgment. This research was supported in part by NATO's Scientific Affairs Division in the framework of the Science for Stability Programme. Partial support of the EPSRC is also acknowledged.

References and Notes

(1) Goodman, I. *Developments in Block Copolymers*; Applied Science: New York, 1982 and 1985; Vols. 1 and 2.
(2) Leibler, L. *Macromolecules* **1980**, *13*, 1602.
(3) Semenov, A. N. *Zh. Eksp. Teor. Fiz.* **1985**, *88*, 1242.
(4) Thomas, E. L.; Alward, D. B.; Kinning, D. J.; Martin, D. S.; Handlin, D. L.; Jr. Fetters, L. J. *Macromolecules* **1986**, *19*, 2197.
(5) Anderson, D. M.; Thomas, E. L. *Macromolecules* **1988**, *21*, 3221.
(6) Thomas, E. L.; Anderson, D. M.; Henkee, C. S.; Hoffman, D. *Nature* **1988**, *334*, 598.
(7) Alward, D. B.; Kinning, D. J.; Thomas, E. L.; Fetters, L. J. *Macromolecules* **1986**, *19*, 215.
(8) Hasegawa, H.; Tanaka, H.; Yamasaki, K.; Hashimoto, T. *Macromolecules* **1987**, *20*, 1651.
(9) Hajduk, D. A.; Harper, P. E.; Gruner, S. M.; Honeker, C. C.; Thomas, E. L.; Fetters, L. J. *Macromolecules* **1995**, *28*, 2570.
(10) Likhtman, A. E.; Semenov, A. N. *Macromolecules* **1994**, *27*, 3103.
(11) Olmsted, P. D.; Milner, S. T. *Phys. Rev. Lett.* **1994**, *72*, 936.
(12) Olmsted, P. D.; Milner, S. T. *Phys. Rev. Lett.* **1995**, *74*, 829.
(13) Semenov, A. N. *Macromolecules* **1993**, *26*, 2273.
(14) Matsen, M. W.; Schick, M. *Phys. Rev. Lett.* **1994**, *72*, 2660.
(15) Matsen, M. W. *Phys. Rev. Lett.* **1995**, *74*, 4225.
(16) Matsen, M. W. *Macromolecules* **1995**, *28*, 5765.
(17) Whitmore, M. D.; Noolandi, J. *Macromolecules* **1985**, *18*, 657. Whitmore, M. D.; Smith, T. W. *Macromolecules* **1994**, *27*, 4673.
(18) Whitmore, M. D.; Noolandi, J. *Macromolecules* **1985**, *18*, 2486.
(19) Xi, H.; Milner, S. T. *Macromolecules* **1996**, *29*, 2404.
(20) Helfand, E.; Wasserman, Z. R. *Macromolecules* **1976**, *9*, 879. Helfand, E.; Wasserman, Z. R. *Macromolecules* **1978**, *11*, 960. Helfand, E.; Wasserman, Z. R. *Macromolecules* **1980**, *13*, 994.
(21) Note that junction points are effectively attached to the interfaces with 2D density, which is determined by the period of the lamellar structure.
(22) Milner, S. T.; Witten, T. A.; Cates, M. E. *Macromolecules* **1988**, *21*, 2610.
(23) Ball, R. C.; Marko, J. F.; Milner, S. T.; Witten, T. A. *Macromolecules* **1991**, *24*, 693.
(24) Note that the experimentally observed window of the bicontinuous phases is normally within the region $f < 0.7$; the same is true for the composition corresponding to the transition between cylindrical and lamellar morphologies as predicted by theories.
(25) Schoen, A. H. NASA Technical Report No. 05541, 1970.
(26) Here we assume that polymer trajectories are straight lines, and also that all polymer blocks "grafted" to a given small interfacial element are nearly parallel.
(27) Bates, F. S.; et al. *Faraday Discuss. Chem. Soc.* **1994**, *98*, 7.

MA9702713